International Journal of Applied Power Engineering (IJAPE)
Vol.6, No.2, August 2017, pp. 113~122
ISSN: 2252-8792 DOI: 10.11591/ijape.v6.i2.pp113-122

New Optimization Method of the MPPT Algorithm and Balancing Voltage Control of the Three-Level Boost Converter (TLBC)

Hassan Abouobaida, Said El Bied
Laboratory of Engineering Sciences for Energy, National School of Applied Sciences of El Jadida, Chouaib-Doukkali University, Morocco

Article Info

Article history:

Received May 15, 2017
Revised Jun 25, 2017
Accepted Jul 18, 2017

Keyword:

MPPT
PMSG
Three Level Boost Converter
Variable Step Size
Voltage Balancing Control

ABSTRACT

This paper is dedicated to studying the control of the Three Level Boost Converters (TLBC) and the optimization method of Maximum Power Point Tracking (MPPT) based a variable step. The main objective of the optimization is to find a compromise between the response time and the amplitude of the oscillations around the optimal point. The nonlinear behavior of the TLBC is manifested by the presence of the disturbances. For reasons of simplicity of the control, a linearization based on the dynamic compensation of the disturbance is proposed. On the one hand, a cascaded MPPT algorithm and a simple linear regulator allow adjusting the inductance current and a maximum power operation of the wind system. On the other hand, a second linear regulator ensures balancing of the output voltages. The paper proposes a new approach to the optimization of the Inc-Cond MPPT. The suggested contribution consists of using an exponential function of the power derivative to develop a variable step. The adoption of the variable step size according to the dynamics of the wind system implies a compromise between the response time and the amplitude of the ripples around the optimal point. The simulation results showed that a variable step size, especially in transient conditions and during a very rapid climate change recover the optimum power point within a reasonable time and suitable amplitude of the oscillations. The results achieved in this study show the ability of the proposed approach to extract the maximum power according to the available wind speed while guaranteeing a better efficiency. The developed study is summarized by the following points: (a) modeling the wind conversion systems, (b) detailing the control approach of the TLBC and presenting the variable step method (c) presenting the simulations results and evaluating the perf

Corresponding Author:

Hassan Abouobaida,
Laboratory of Engineering Sciences for Energy,
National School of Applied Sciences of El Jadida,
Chouaib-Doukkali University, Morocco.
Email: hassanabouobaida@gmail.com

1. INTRODUCTION

The power wind conversion system consists of a synchronous generator a (PMSG), a three-phase uncontrolled diode rectifier and a three-level boost converter. The structure studied is illustrated in Figure 1.

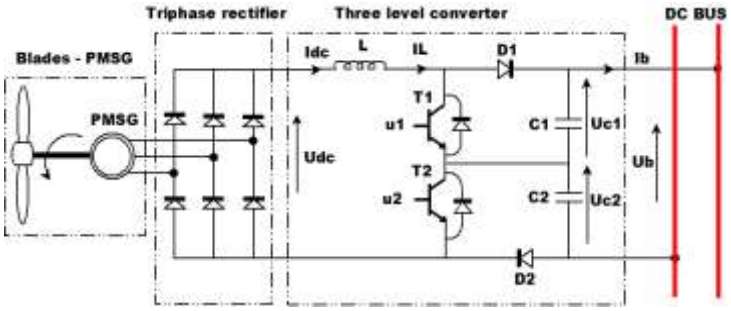

Figure 1. Power wind conversion system based PMSG generator and the three-level Boost converter TLBC

1.1. The turbine model

The aerodynamic power P_t captured by the wind turbine is expressed by the following relation [1]

$$P = \frac{1}{2}\pi.\rho.R^2.Cp(\lambda).v^3 \quad (1)$$

Where the tip speed ratio λ is given by

$$\lambda = \frac{R.\Omega_m}{v} \quad (2)$$

v is the wind speed, ρ is the air density, R is the rotor radius and Cp is the power coefficient. The power coefficient is expressed as function of tip speed ratio λ in place of pitch angle β as

$$C_p = 0.576.\left(\frac{116}{\lambda_i} - 0.4\beta - 5\right).e^{\frac{21}{\lambda_i}} + 0.0068.\lambda \quad (3)$$

$$\frac{1}{\lambda_i} = \frac{1}{\lambda + 0.08\beta} - \frac{0.035}{\beta^3 + 1} \quad (4)$$

The aerodynamic power is also defined by

$$P = T_m\,.\,\omega_m \quad (5)$$

Where T_m is the aerodynamic torque and ω_m is the rotor speed. The curve of power in term of the rotor speed and the aerodynamic power in term of the tip speed ratio are illustrated in Figure 2 and Figure 3 respectively.

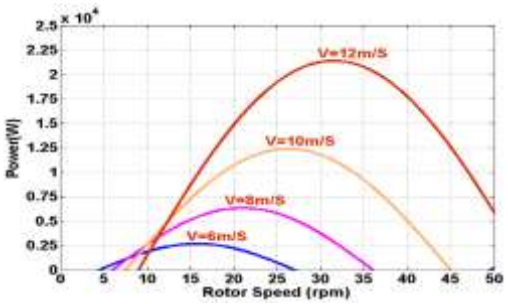

Figure 2. Curve of power of the wind

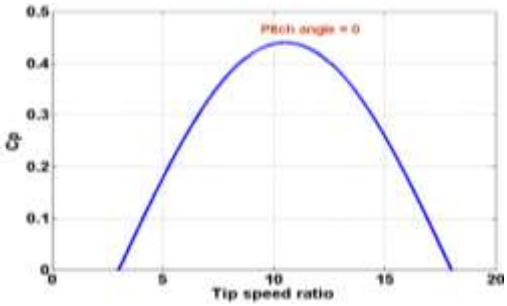

Figure 3. The power coefficient as function of tip speed ratio

In this work, the control of the wind conversion system is carried out keeping the pitch angle equal to zero (β=0). The following mechanical model gives the dynamic of the wind turbine

$$J\frac{d\omega_m}{dt} = T_m - T_{em} - f.\omega_m \quad (6)$$

Where $T_{em}$the electromagnetic torque of the synchronous generator, J is the turbine total inertia and f is the turbine total external damping.

1.2. The PMSG model

The dynamic equations of a (PMSG) generator is written in a synchronously rotating *dq* reference frame as [1]

$$V_{sd} = -R_s.i_{sd} - L_d \frac{di_{sd}}{dt} + L_q.\omega_r.i_{sq} \quad (7)$$

$$V_{sq} = -R_s.i_{sq} - L_q \frac{di_{sq}}{dt} - L_d.\omega_r.i_{sd} + \sqrt{\frac{3}{2}}.\Phi_{st}.\omega_r \quad (8)$$

Where V_{sq} and V_{sd} are the *q*-axis and *d*-axis stator terminal voltages. i_{sd} and i_{sq} are the *q*-axis and *d*-axis stator currents, R_s is the resistance of the stator windings, $\omega_r = p.\omega_m$ is the electrical angular velocity of the rotor and p is the number of pole pairs of the (PMSG). Φ_{st} is the flux linkage produced by the permanent magnet mechanism located in the rotor.

The power produced by (PMSG) generator can be expressed as a function of the dq components of currents and the dq components of the voltage according to the following relation:

$$P = \frac{3}{2}.(V_{sd}I_{sd} + V_{sq}I_{sq}) \quad (9)$$

1.3. Three-level boost converter model

The four possibilities of the switching states of the power switches are illustrated in Figure 4 [2-9]:

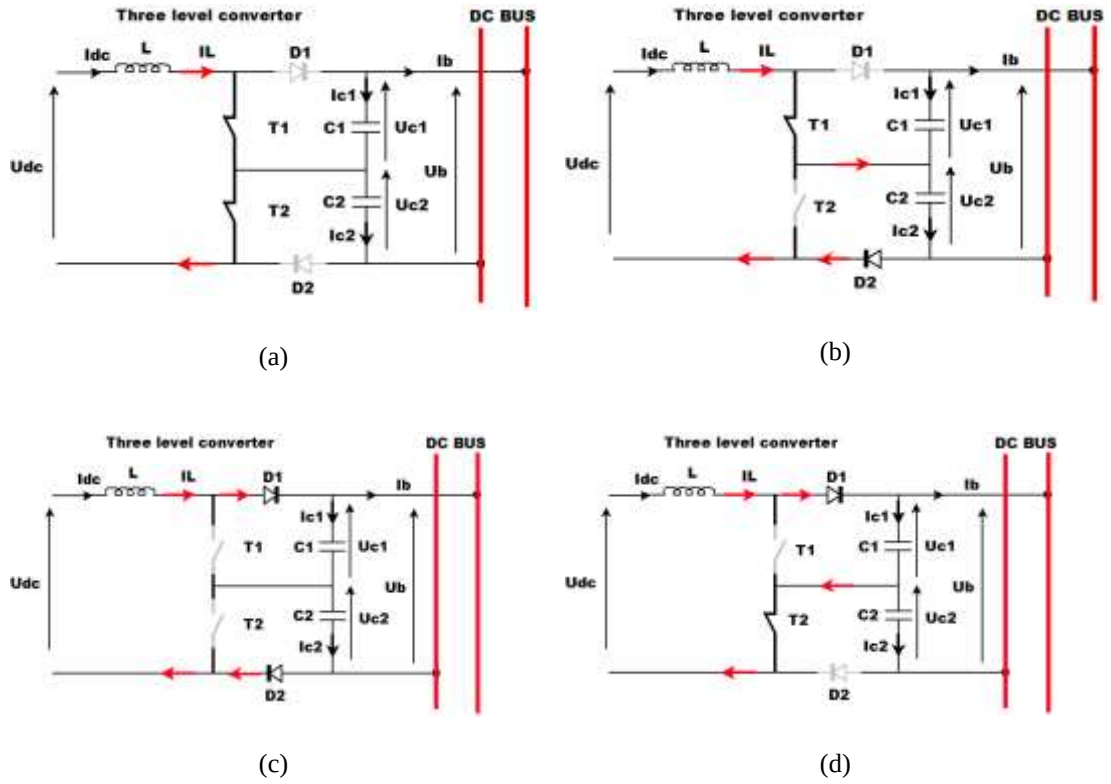

Figure 4. Possible switching states in three-level boost converter: (a) state 1; (b) state 2; (c) state 3; and (d) state 4

The dynamics model of the TLBC is expressed by the following equations:

$$\dot{x} = A.x + B \quad (10)$$

By replacing x, A and B with their expressions, the dynamics of the converter TLBC can be modeled by the following matrix:

$$\begin{bmatrix} \dot{U}_{c1} \\ \dot{U}_{c2} \\ \dot{I}_L \end{bmatrix} = \begin{bmatrix} 0 & 0 & \frac{u_1}{C_1} \\ 0 & 0 & \frac{u_2}{C_2} \\ -\frac{u_1}{L} & -\frac{u_2}{L} & 0 \end{bmatrix} \begin{bmatrix} U_{c1} \\ U_{c2} \\ I_L \end{bmatrix} + \begin{bmatrix} \frac{-I_b}{C_1} \\ \frac{-I_b}{C_2} \\ \frac{U_{dc}}{L} \end{bmatrix} \quad (11)$$

where L, I_L and I_b are the storage inductance, the current across it and the output current. U_{dc}, U_{C1} and U_{C2} are the output voltage of the three-phase rectifier and the voltage of the capacitors C1 and C2. u1 and u2 are respectively the control signal of the two power switches T1 and T2 [10].

2. CONTROL APPROACH OF THE TLBC

The objectives of controlling the three-level boost converter levels are [2]:

a. Balancing the two voltages at the output of the converter.
b. Extraction of maximum power from the wind generator.

The adjustment loops are constructed according to the following hypothesis:

a. The output voltage of the TLBC is assumed to be constant. The regulation of this tension is ensured by another control loop (part not studied in this paper).
b. The voltage balancing loop of Uc1 and Uc2 is faster than the current adjustment loop IL. In closed loop, the loop of the voltages is designed to be faster than the current loop which allows a very fast convergence of the difference Uc1-Uc2 to zero.

Using the average equivalent model, the TLBC converter is represented in the open loop by the system as shown in Figure 5.

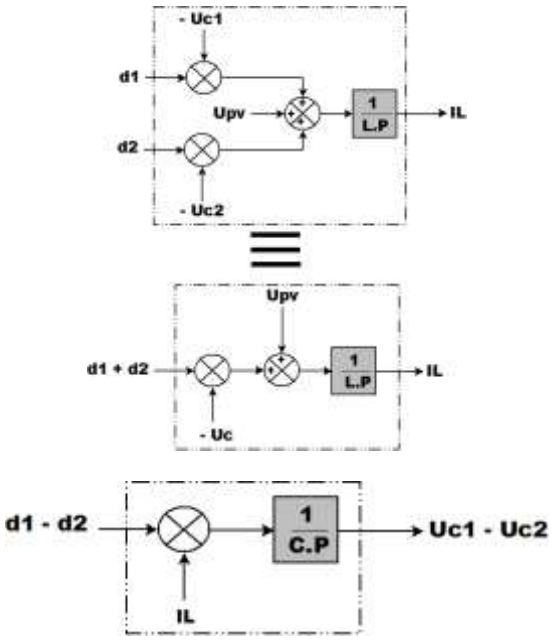

Figure 5. Open-loop representation of the TLBC converter

where d1 and d2 are Are respectively the average value in a cutting period of the command u1 and the command u2. According to the above-mentioned hypothesis, the voltages Uc1 and Uc2 are well maintained equal (Uc1=Uc2=Uc). IL, Uc and Udc are considered disturbances which must be compensated during a closed-loop control.

The control of the difference Uc1-Uc2 and the current IL is reduced to a first order system. A simple PI controller is used to:

a. Balancing the two voltages of the two capacitors at the output of the TLBC,
b. The adjusting the current IL which allows a maximum power point operation of the wind system.

Figure 6 summarizes the control approach used [2]-[11]:

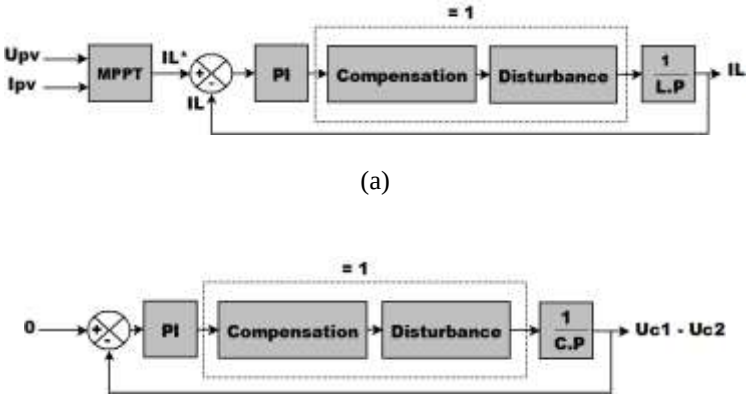

Figure 6. Closed loop control, (a) Current control approach, (b) balancing voltage control

3. INC-COND MPPT BASED A FIXED AND VARIABLE STEP SIZE

3.1. Inc-cond MPPT based a fixed step size

The conventional Inc-Cond MPPT is based on a constant step. Figure 7 illustrates the operating principle of the conventional Inc-Cond MPPT:

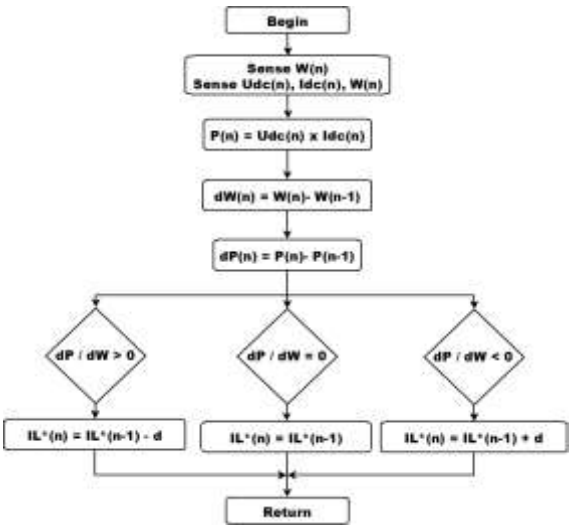

Figure 7. Conventional Inc-Cond MPPT

A relatively large step leads to oscillations of great amplitudes and a very interesting tracking time. A very small step will lead to a very long tracking time and very limited oscillations around a desired point.

3.2. Proposed inc-cond MPPT based variable step size

Finding a compromise between the response time (search time or tracking time) and the amplitude of the ripple is the expected goal of this work. To achieve this objective, the Inc-Cond algorithm is realized based on a variable step size function of the dynamics of the wind system. Figure 8 illustrates the operating principle of the proposed Inc-Cond MPPT:

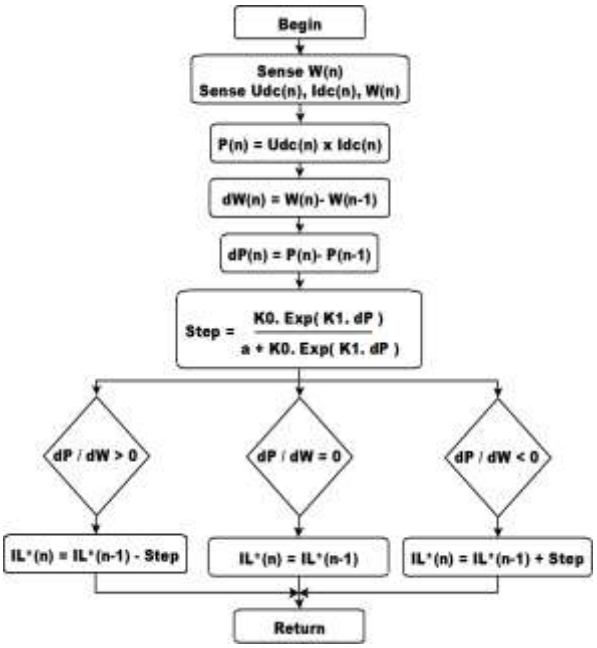

Figure 8. Principle of the INC-cond MPPT based a variable step size

4. SIMULATION RESULTS

The model of the power wind conversion system, three-level boost converter TLBC and the proposed Inc-Cond MPPT are implemented in Matlab/Simulink. In this study, the wind generator delivers a maximum power of 22kwatts. The specification of the control parameters and the main characteristics of the wind system are summarized in Table 1 and Table 2 respectively.

Table 1. Parameters Used in the Simulation

	Parameters	Value	Unit
Three	L	2	mH
Level	C1	470	µF
Boost	C2	470	µF
Converter	f	20k	Hz
Inc-Cond MPPT	Step	0.001	-

Table 2. Main characteristics of the Wind turbine and PMSG

	Parameters	Value	Unit
Turbine	Vt_n	12	m/s
	R	4	m
PMSG	U_s	500	V
	P_n	22 k	W
	f	50	Hz
	R_s	50 m	Ω
	L_d=L_q	0.6 m	H
	J_m	0.011	$kg.m^2$
	P	10	-

In order to prove the validity of the control approach and the efficiency of the proposed optimization algorithm, the simulation results of the conventional Inc-Cond algorithm and the proposed algorithm will be presented, discussed and compared. A wind profile is applied to the wind turbine blades as illustrated in Figure 9(a). Firstly, the simulation results are given for Inc-Cond MPPT based a constant step. Figure 9(b) shows the inductance current and its reference. According to this figure, the inductor current is well regulated to its reference. According to this figure, in transient mode, the inductance current reaches its reference point after 0.36 seconds. During an abrupt change in wind speed, the inductance current took about 0.7 seconds to

reach its reference. Figure 10(c) shows an inductor current zoom. According to this figure, the amplitude of the ripple of the inductance current is 0.6A. Figure 9(d) illustrates the power delivered by the wind system as a function of time. By comparing the extracted power according to the wind speed and the maximum power given by Figure 2, it is noted that the wind system operates at its maximum power. Figure 9(e) shows the wind power coefficient. According to Figure 3, the optimal value of this factor is 0.45. The control of the wind system for maximum power operation made it possible to adjust this factor to its optimum value. It is noted that the power coefficient deviates from its optimum value during the change of wind speed, but the control was able to reset this factor to its optimal value for 0.6 seconds. Figure 9(f) shows the voltages of the capacitors at the output of the converter. According to this figure, it can be seen that these two voltages are well balanced. At the moment of change of the wind speed, a very negligible difference appears between these two voltages, and then the control acts quickly to maintain balancing these voltages again.

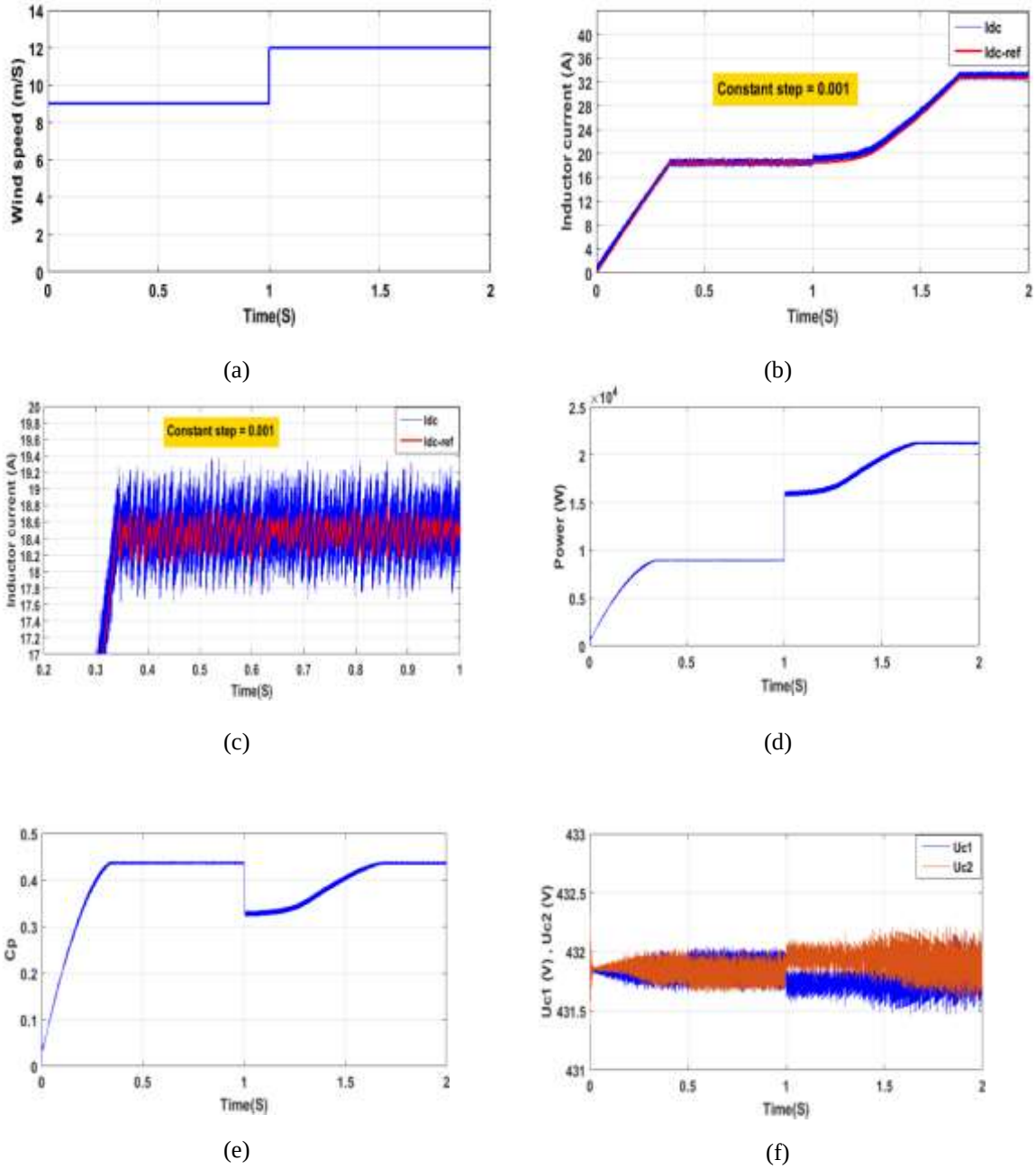

Figure 9. Inc-cond MPPT results based constant step (Step=0.001), (a) Wind speed (m/S), (b) Inductor current (A), (c) Inductor current zoom (A), (d) Power (W), (e) Power coefficient, (f) Capacitor voltages(V)

In order to compare the proposed approach based on a variable step to the conventional Inc-Cond MPPT presented in the previous results, the same wind speed profile is applied to the wind system. Figure 10 gives the simulation results of the control of the TLBC using the optimized MPPT.

Figure 10(b) shows the inductance current and its reference. According to this figure, the inductor current is well regulated to its reference. In the transient mode, the inductance current reaches its reference point after 0.12 seconds. During an abrupt change in wind speed, the inductance current took about 0.12 seconds to reach its reference. According to these results, it is noted that the transient time and the tracking time are well improved compared to the time taken by the conventional MPPT Inc-Cond.

Figure 10(c) shows an inductor current zoom. The amplitude of the ripple of this current is very limited. According to this figure, the amplitude of the ripples around the optimum point is well maintained less than or equal to 0.5 A. Figure 10(d) illustrates the power delivered by the wind system as a function of time. According Figure 2, it is noted that the wind system operates at its maximum power.

Figure 10(e) shows the wind power coefficient. In the transient mode, the power coefficient reaches its optimal value equal to 0.45 after 0.12 seconds. It is noted that power coefficient deviates from its optimum value during the change of wind speed, but the control resets this factor to its optimal value for 0.1second.

Figure 10(f) shows the voltages of the capacitors at the output of the converter. According to Figure 10(f), the voltages Uc1 and Uc2 are well balanced. At the moment of change of the wind speed, a very negligible difference appears between these two voltages, and then the control acts quickly to maintain balancing these voltages again.

Figure 10(g) shows the step value used for determining the optimum inductance current value. It is noted that this step takes on a very important value in transient mode or during a change in wind speed. This step tends quickly to a very low value when the system finds the optimal point.

Figure 10(h) shows in zoom the step used by the MPPT Inc-Cond. According to this figure, the variation of step size during the changes in wind speed or in transient conditions made it possible to detect the optimum point more quickly. When the optimum point is found, the system oscillates around this point with very limited amplitude ripples, which is justified by the presence of the smaller step size in the established regime.

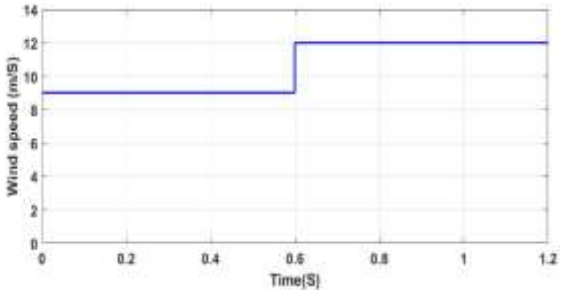

(a)

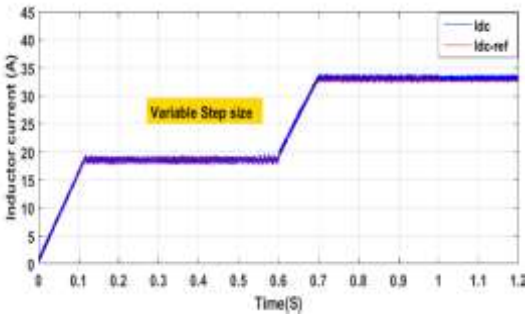

(b)

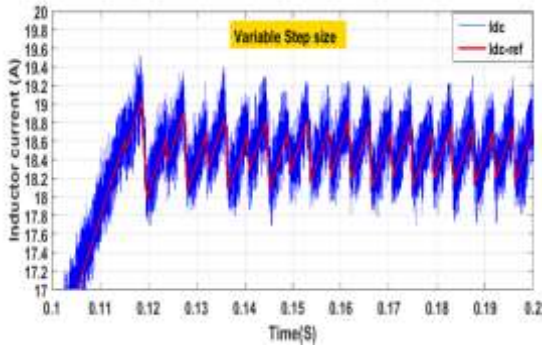

(c)

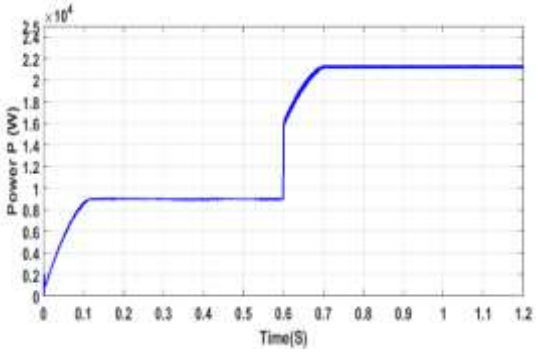

(d)

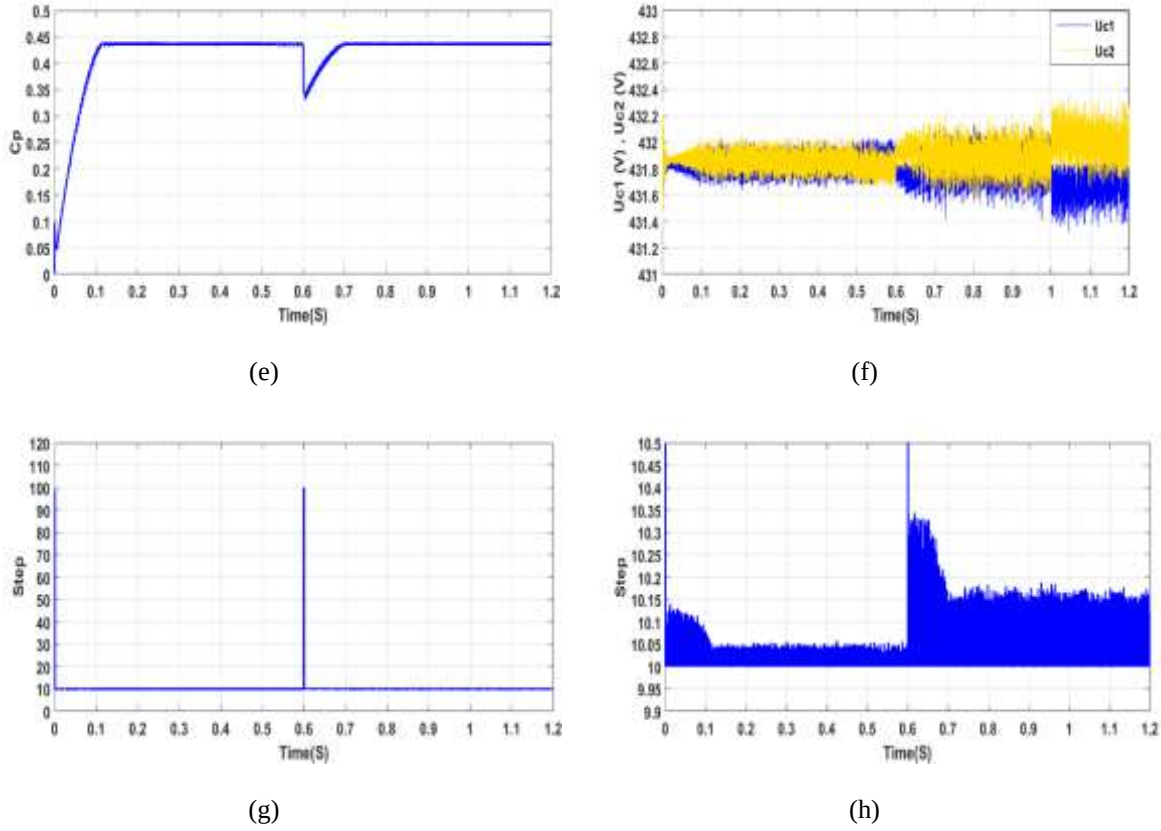

(e) (f)

(g) (h)

Figure 10. Inc-cond MPPT results based variable step(Step), (a) Wind speed (m/S), (b) Inductor current (A), (c) Inductor current zoom (A), (d) Power (W), (e) Power coefficient, (f) Capacitor voltages (V), (g) Step size, (h) Step size zoom

The simulation results indicate that:

a. The voltages of the capacitors are kept equal. Based on the results, it can be deduced that the balancing of the output voltages of the TLBC is assured,
b. The power extracted is identical to the value given by the theoretical power curve according to the wind speed. The maximum power operation and the adjustment approach of the inductance current are validated.
c. The search time and the tracking time are improved in the proposed approach. The improved MPPT takes the little time (0.12 S instead of 0.36S) to recover the optimal point.
d. The amplitude of the ripples around the optimal point is well maintained at a maximum which does not exceed 0.5A which justify the validity of the proposed method.

5. CONCLUSION

The paper addressed the modeling and control of the TLBC. The control approach is based on linearization and disturbance compensation since the three-level boost converter exhibits non-linear behavior. The objectives fixed by the control are respectively balancing the voltages of the capacitors and extracting the maximum power. On the one hand, according to the simulations results, it is noted that the control and linearization approach is well validated and the wind system is operating at its maximum power. On the other hand, the optimization approach of the Inc-Cond MPPT is validated since the transient time and the tracking time are well minimized and the ripple around the optimal point is well maintained at a reasonable limit.

REFERENCES

[1] H. Abouobaida and E. Beid Said, "New MPPT control for wind conversion system based PMSG and a comparaison to conventionals approachs," *2017 14th International Multi-Conference on Systems, Signals & Devices (SSD)*, Marrakech, 2017, pp. 38-43.

[2] H. Chen and W. Lin, "MPPT and Voltage Balancing Control With Sensing Only Inductor Current for Photovoltaic-Fed, Three-Level, Boost-Type Converters," in *IEEE Transactions on Power Electronics*, vol. 29, no. 1, pp. 29-35, Jan. 2014.
[3] Said El Beid, Hassan Abouobaida, Abdelowahed Hajjaji, "TS Fuzzy Modeling Appoach for the Three Level Boost Converter," *The International conference on Advanced Materials for Photonics, Sensing and Energy AppliCAtions (AMPSECA' 2017)*, 2017
[4] Hassan Fathabadi, "Novel high efficient speed sensorless controller for maximum power extraction from wind energy conversion systems," *Energy Conversion and Management*, vol. 123, pp. 392-401, September 2016.
[5] Y. Zhao, C. Wei, Z. Zhang and W. Qiao, "A Review on Position/Speed Sensorless Control for Permanent-Magnet Synchronous Machine-Based Wind Energy Conversion Systems," in *IEEE Journal of Emerging and Selected Topics in Power Electronics*, vol. 1, no. 4, pp. 203-216, Dec. 2013.
[6] A. Urtasun, P. Sanchis and L. Marroyo, "Small Wind Turbine Sensorless MPPT: Robustness Analysis and Lossless Approach," in *IEEE Transactions on Industry Applications*, vol. 50, no. 6, pp. 4113-4121, Nov.-Dec. 2014.
[7] Zhang X, Li Q, Yin M, Ye X, Zou Y, "An improved hill-climbing searching method based on halt mechanism," In *Zhongguo Dianji Gongcheng Xuebao/Proceed Chin Soc Electr Eng*, pp. 128–34, 2012
[8] L. A. Vitoi, R. Krishna, D. E. Soman, M. Leijon and S. K. Kottayil, "Control and implementation of three level boost converter for load voltage regulation," *IECON 2013 - 39th Annual Conference of the IEEE Industrial Electronics Society*, Vienna, 2013, pp. 561-565.
[9] H. Chen and W. Lin, "Three-level boosting MPPT control with reduced number of sensors," *2013 4th IEEE International Symposium on Power Electronics for Distributed Generation Systems (PEDG)*, Rogers, AR, 2013, pp. 1-6.
[10] M. D. Bougrine, A. Benalia and M. H. Benbouzid, "Simple sliding mode applied to the three-level boost converter for fuel cell applications," *2015 3rd International Conference on Control, Engineering & Information Technology (CEIT)*, Tlemcen, 2015, pp. 1-6.
[11] J. Kwon, B. Kwon and K. Nam, "Three-Phase Photovoltaic System With Three-Level Boosting MPPT Control," in *IEEE Transactions on Power Electronics*, vol. 23, no. 5, pp. 2319-2327, Sept. 2008.